Pseudogap of liquid Tl_2Te

Melvin Cutler
Physics Department, Oregon State University, Corvallis, Oregon 97331
(Received 10 August 1973)

Analysis of experimental curves for the electrical conductivity σ and thermopower S of Tl_xTe_{1-x} alloys near the composition Tl_2Te has yielded a quantitative description of the pseudogap. A model expressed in terms of two bands with a negative temperature coefficient for the band gap has been fitted with parameters which yield very good agreement with the experimental curves. The theoretical expressions for S and σ are based on the diffusive mechanism for transport, according to which the conductivity at a given energy $\sigma(E)$ is proportional to the square of the density of states $N(E)$. The effect of the mobility shoulder is to cut off $\sigma(E)$ at the mobility edges. For the conduction band, it is found that the density of states $N_c(E)$ is parabolic. The mobility edge E_{c1} is within kT of the band edge E_{c0}, and is therefore not experimentally discernible. For the valence band, the results are more ambiguous. A parabolic density of states $N_v(E)$ yields fairly accurate results, and we deduce a value ≈ 0.20 eV for the distance of the mobility edge E_{v1} from the band edge E_{v0}, but there are some uncertainties associated with both of these results. At $T > 770$ °K, the band gap becomes negative. In accordance with Mott's observation that localized and nonlocalized states cannot overlap in energy, our model takes $\sigma(E) \propto [N_c(E) + N_v(E)]^2$, and localized valence-band states become conducting when their energies rise above the conduction-band mobility edge.

I. INTRODUCTION

The designation liquid semiconductor in itself implies the occurrence of a band gap, or at least a minimum in the density of states near the Fermi energy, which is commonly called a pseudogap. Yet there is very little experimental work which has yielded quantitative information about the band gaps of liquid semiconductors. This has been a source of embarrassment for workers in this field, and it also presents a challenging problem. The purpose of this paper is to present an analysis of existing transport data for thallium-tellurium alloys which has yielded a quantitative description of the density of states in the vicinity of the pseudogap which applies to compositions near Tl_2Te. This represents, we believe, the first complete description of the pseudogap in a liquid semiconductor. The results also provide new insights about some features of pseudogaps which are of general importance for disordered materials.

One naturally looks to measurements of optical absorption or reflection for information about the band gap of semiconductors. There is very little information of this sort for liquid semiconductors, possibly because of experimental difficulties and the limited information generated by data at high temperatures. Tl-Te alloys have not been studied optically. Liquid tellurium has been studied and shows a slight indication of a minimum in the density of states.[1] The curve for the conductivity versus frequency differs only by a factor of 2 between the maximum and minimum values. Much clearer information is provided by absorption curves for As_2Se_3, which have been measured both in the liquid and vitreous phases.[2] The distinct absorption edge of the glass at low temperatures shifts to longer wavelengths with reduced slopes as the temperature is increased above the softening point, which suggests a decrease in width and a smearing of the pseudogap. Because the absorption follows a modified form of the Urbach rule whose interpretation is open to question, it has been difficult to make a precise interpretation of these data. But a temperature coefficient for the band gap of the liquid was determined to be -1.7×10^{-3} eV/°K, and this is in accord with the coefficient derived from the thermopower assuming ambipolar transport.[2,3] Points of interest about these results, in relation to our work, are that there is a large negative temperature coefficient of the band gap (compared to crystalline solids), as is common among chalcogenide glasses, and that the band gap for liquid As_2Se_3 seems to go to zero at about 1000 °K. Another liquid semiconductor which has been studied optically is CdTe.[4] This also shows evidence of a band gap with a strong temperature dependence.

Transport measurements provide another possible source of information about the pseudogap. In many binary alloys which are liquid semiconductors, the isotherms for the resistivity ρ have a peak at a characteristic composition, and among these the thermopower S frequently changes sign near that composition. As an example of particular interest, the isotherms of ρ and S are shown for Tl_xTe_{1-x} in Fig. 1. The peak in ρ occurs at $x = \frac{2}{3}$, corresponding to a composition Tl_2Te, which indicates that the Fermi energy E_F is near the center of the pseudogap at this composition. The sign and magnitude of the thermopower indicates that E_F is in the conduction band for thallium-rich alloys

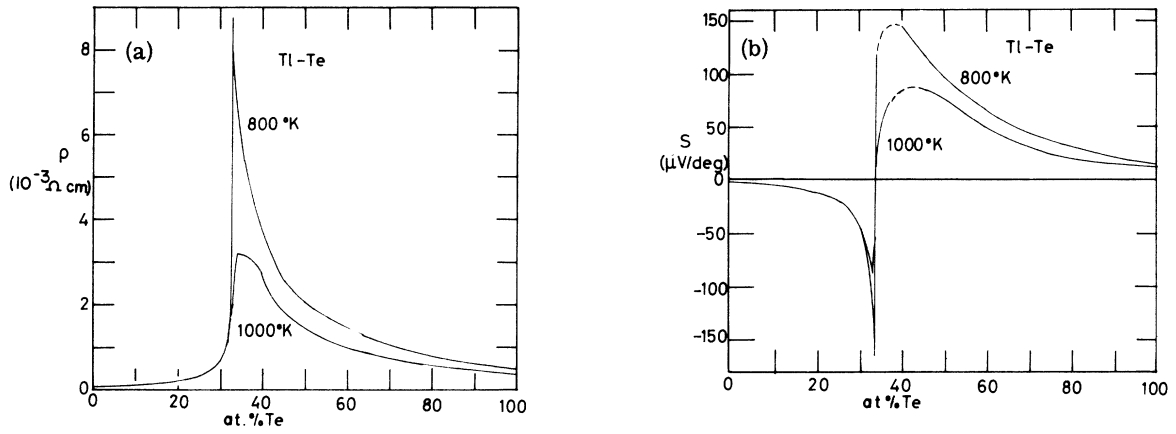

FIG. 1. Isotherms for the resistivity ρ and the thermopower S of Tl-Te at temperatures 800 and 1000°K. (From Ref. 7.)

($x > \frac{2}{3}$), and for tellurium-rich alloys E_F is in the valence band. Although analysis of the behavior of ρ and S has yielded information about these two bands, [5-7] the existence of the pseudogap is indicated only indirectly. In order to study the pseudogap, one must examine data reflecting excitations between the bands. Changes in slope of $\rho(T)$ and $S(T)$ which are caused by such excitations at composition near Tl_2Te have been noted in past work. [5,6,8] But quantitative examination of these data has been inhibited in the past by the absence of sufficient theoretical information about the electronic structure and transport behavior. This is particularly needed since we must study small deviations in the form of these curves from the "extrinsic" one which are caused by thermal excitation of electron-hole pairs.

In recent years, important progress has been made in understanding the electronic structure and transport behavior of disordered systems, and this has provided the needed tools for studying the pseudogap of Tl_2Te, as will be set forth in this paper. We shall conclude this section by reviewing briefly these concepts, [9] and show in later sections how our model for the pseudogap is derived.

The key element in the theory is the density-of-states curve $N(E)$, which contains a dip (the pseudogap) between two maxima which correspond to the valence and conduction bands, as shown in Fig. 2(a). This electronic structure can be regarded as being generated from a metallic system as the result of strong interactions between the ions and the electrons. Alternatively, one can start with covalently bound atoms in discrete molecules with discrete energy levels, and these give rise to bands as the result of broadening due to mutual interactions. Both models arrive at the same density-of-states curve. [7] It will be convenient for us to use the latter point of view, since we describe the pseudogap in terms of a two-band model. Thus we conceive the density of states as arising from two discrete bands which overlap as shown by the dashed lines in Fig. 2(a).

For crystalline material, the band edge is usually parabolic, since it represents a simple minimum of the energy in wave-vector space. This result may also be reasonably expected in materials with long-range disorder in the absence of potential fluctuations. Band tailing and distortion of the band edge are believed to be caused by fluctuations in potential, [10] but the complexity of the theory for band tailing discourages attempts at making predictions of its magnitude and shape for liquid semiconductors.

A second effect of the potential fluctuations is that if $N(E)$ in the pseudogap is low enough, there will be a range of energy within which all the electronic states are localized, and beyond which the electronic states extend throughout the volume, as shown in Fig. 2(a). This phenomenon, called Anderson localization, was deduced by Mott [11] by an

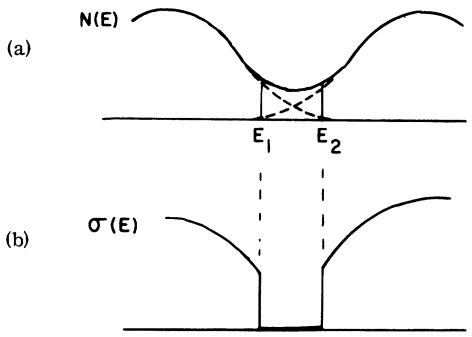

FIG. 2. (a) Density of states $N(E)$ and (b) conductivity $\sigma(E)$ in the pseudogap model. The states are localized between energies E_1 and E_2.

extension of theoretical results obtained by Anderson.[12] According to Mott's discussion the energy at which the localization occurs, called the mobility edge, depends primarily on the magnitude of $N(E)$, but this dependence is affected by the coordination number and the character of the atomic wave functions from which the final states are derived. There has been considerable discussion and incomplete agreement about the existence of the mobility edge, and the nature of transport at energies in its vicinity.[13]

The localized states are expected to have a mobility smaller than that of the extended states by several orders of magnitude. This is because transport is by hopping for localized states with a characteristic frequency no larger than that of the atomic vibrations ($\sim 10^{12}$ sec^{-1}). On the other hand, the electrons in the extended states near the transition energy are believed to move with a similar mean free path of the order of the interatomic distance, but with a characteristic frequency of the order of E_b/h, where E_b is the bandwidth, which gives $\sim 10^{15}$ sec^{-1}. The resulting drop in mobility for the localized states, first pointed out by Cohen,[14] has led to the name "mobility edge" for the transition energy. As a result of the Anderson transition, the conductivity considered as a function of energy, $\sigma(E)$, has a shape indicated in Fig. 2(b). For many liquid semiconductors, and certainly in the case of Tl_2Te, the large value of kT compared to the distance between the mobility edges, together with the relatively low conductivity of the localized states, ensure that transport will be predominantly due to carriers thermally excited to the extended states near the mobility edges. Consequently, it will be a good approximation to assume that $\sigma(E) = 0$ between the mobility edges.

Above the mobility edges, transport is believed to proceed in the extended states with a mean free path equal to the interatomic distance. Mott has developed a model[15] for this in which the electron wave function is scattered incoherently within this distance, with the result that

$$\sigma(E) = A[N(E)]^2, \tag{1}$$

where A is a constant. A more detailed derivation for this "diffusive" mechanism is provided in a paper by Hindley.[16] The validity of the theory for diffusive transport is strongly supported by NMR studies of liquid semiconductors by Warren.[17] This work also supports Mott's estimate that the diffusive mechanism provides an appropriate description for extended states when $\sigma(E) \lesssim 2500$ Ω^{-1}cm^{-1}. We shall use Eq. (1) with a mobility shoulder cutoff as our basic equation for examining the transport behavior of Tl-Te alloys.

II. MONOPOLAR TRANSPORT IN THE CONDUCTION BAND FOR THALLIUM-RICH COMPOSITIONS

A. Extrinsic behavior

In previous work[5,6] the behavior of σ and S as a function of x (the composition parameter in Tl_xTe_{1-x}) and to a lesser extent as a function of T was explained in terms of a model where a constant density of electrons n_0 is generated by complete ionization of Tl atoms in excess of the composition Tl_2Te. In the absence of an appropriate theory of transport, conventional transport theory was used which is predicated on a long mean free path. But it is easy to recast the results in terms of the theory for diffusive transport [Eq. (1)].

One can derive the electrical conductivity and the thermopower from $\sigma(E)$ by the formulas[18]

$$\sigma = -\int_{-\infty}^{\infty} \sigma(E)\frac{\partial f}{\partial E}\,de \tag{2}$$

and

$$S = \frac{k}{e}\int_{-\infty}^{\infty} \frac{\sigma(E)}{\sigma}\frac{\partial f}{\partial E}\frac{E-E_F}{kT}\,dE, \tag{3}$$

where f is the Fermi-Dirac distribution function:

$$f = (1+e^{(E-E_F)/kT})^{-1}.$$

Cutler and Field (CF)[5] found that if $\sigma(E)$ is taken to be proportional to E^r, the predicted relation be-

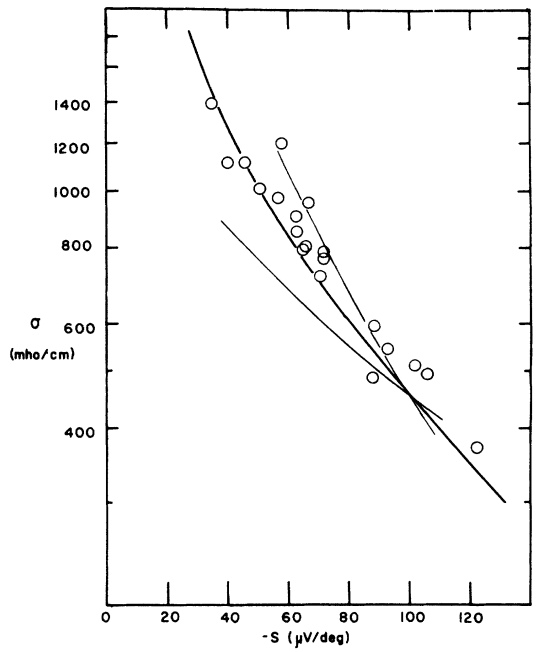

FIG. 3. Comparison of theoretical curves with experimental data for $\ln\sigma$ vs S at $T = 800$°K. The heavy line is for $r = d\ln\sigma(E)/d\ln E = 1$, and the light lines are for $r = \frac{1}{2}$ and $\frac{3}{2}$. (From Ref. 5.)

tween σ and S at constant $T(=800\,^\circ\mathrm{K})$ as the electron density is varied is obeyed very well for $r=1$. Figure 3 shows a comparison of experimental points with theoretical curves with $r=\frac{1}{2}$, 1, and $\frac{3}{2}$. In the context of the theory for diffusive transport [Eq. (1)] and the expected occurrence of a mobility shoulder, this result shows that (a) the density of states for the conduction band $N_c(E)$ is parabolic, so that we can write

$$N_c(E)=C_n(E-E_{c0})^{1/2}, \tag{4}$$

and (b) the mobility edge E_{c1} is close to the edge E_{c0} and band tailing is negligible on a scale determined by kT (~ 0.07 eV). Consequently, our model for transport in the conduction band, in current terms, is derived by substituting Eqs. (1) and (4) into Eqs. (2) and (3), and setting the lower limits to the integrals at E_{c0} (which we assume to be the same as E_{c1}).

This results in a single-band extrinsic solution for transport which can be expressed in terms of Fermi-Dirac integrals $F_n(\xi)$:

$$\sigma=AC_n^2\,kTF_0(\xi), \tag{5}$$

$$S=-(k/e)[2F_1(\xi)/F_0(\xi)-\xi], \tag{6}$$

where

$$\xi=(E_F-E_{c0})/kT \tag{7}$$

and

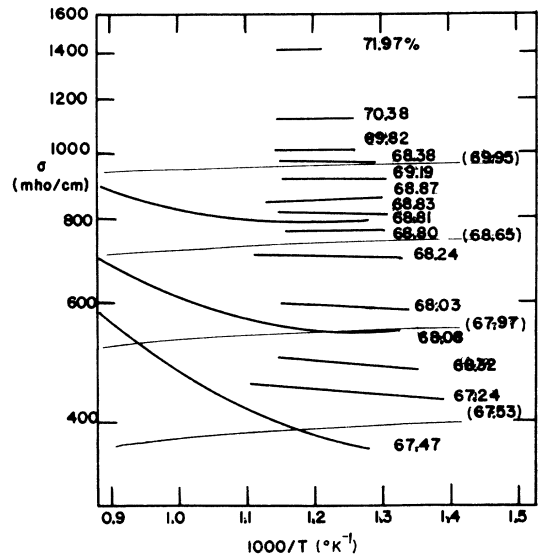

FIG. 4. Experimental curves (heavy lines) for $\sigma(T)$ at various compositions of Tl_xTe_{1-x} are compared to theory (light lines) for a constant electron density. The compositions are labeled by the values of $100x$, and the values for the theoretical curves are enclosed in parentheses. (From Ref. 5.)

$$F_n(\xi)=\int_0^\infty \frac{x^n}{e^{x-\xi}+1}\,dx. \tag{8}$$

The heavy curve ($r=1$) in Fig. 3 corresponds to the theoretical curve obtained by eliminating ξ between Eqs. (5) and (6), and setting $AC_n^2k=0.2275$ $(\Omega\ \mathrm{cm}\ ^\circ\mathrm{K})^{-1}$.

The value of ξ is determined by the electron density n through the formula

$$n=\int_{E_{c0}}^\infty fN_c(E)\,dE=C_n(kT)^{3/2}F_{1/2}(\xi). \tag{9}$$

When the electron density is governed by the charge density of Tl ions, it is given by the formula

$$n_0=3z(x-\tfrac{2}{3})N_a, \tag{10}$$

where N_a is the atom density (2.7×10^{22} cm^{-3}) and z is the charge of the Tl ions. In CF, the value of z was found erroneously to be 3; the correct value is 1.[19] By comparison with experiment of the theoretical curve from Eqs. (6), (9), and (10) for the dependence of S on x at $T=800\,^\circ\mathrm{K}$, described in CF, one arrives at a value of $C_n=1.49\times10^{22}\,\mathrm{eV}^{-3/2}\,\mathrm{cm}^{-3}$. This corresponds to an effective-mass ratio $m_n^*/m=1.68$ if a particle-in-the-box model is used to arrive at C_n in Eq. (4).

B. Effect of electron-hole excitations on n

Equations (5), (6), and (9) predict the effect of temperature on σ and S for a given value of n. If n is assumed to be independent of T and equal to the value n_0 derived from the composition [Eq. (10)], a series of theoretical curves is obtained for S and σ for different compositions.[5] These are compared with experiment in Fig. 4 and 5. It is seen that there are deviations which increase in magnitude with increasing T and as x approaches the intrinsic value $\frac{2}{3}$. The deviations are in the direction expected if electron-hole excitations occur.

A surprising feature of these results is the fact that the deviations for σ and S are similar in relative magnitude for a given T and x. If there is bipolar (ambipolar) transport with electrons (subscript n) and holes (subscript p) having comparable mobilities so that $\Delta\sigma_n\sim\sigma_p$, then for a relatively small density of electron-hole pairs where $\Delta\sigma/\sigma\cong\sigma_p/\sigma$, the corresponding change in S is given by $\Delta S/S=(\sigma_p/\sigma)(S_p-S_n)/S$. Since $(S_p-S_n)/S$ can be expected to be large compared to 1, one expects $\Delta S/S$ to be considerably larger than $\Delta\sigma/\sigma$.

A likely explanation is that the distance of the mobility edge from the band edge in the valence band is greater than it is for the conduction band. Although we have concluded that $E_{c1}-E_{c0}\lesssim kT$, this may not be so for $E_{v0}-E_{v1}$. In such a situation, most of the holes of the electron-hole pairs would be in localized states, so that $\sigma_p\sim0$, whereas the

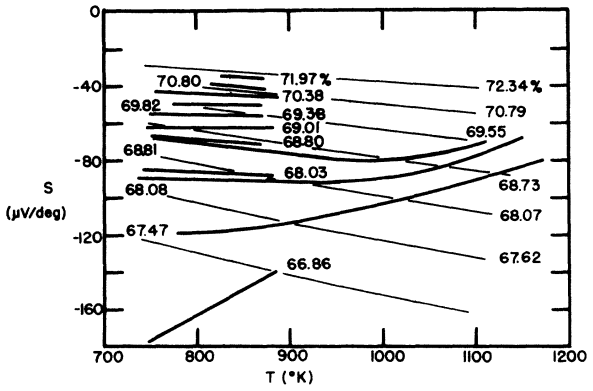

FIG. 5. Experimental curves (heavy lines) for $S(T)$ for various compositions of Tl_xTe_{1-x}, in comparison with theory (light lines) for a constant electron density. The compositions are labeled by $100x$. The values on the right-hand side of the figure refer to the theoretical curves. (From Ref. 5.)

thermally excited electrons are in extended states above E_{c1}. As a consequence, the change on σ and S with T would reflect transport entirely in the conduction band, so that σ and S continue to be described by Eqs. (5) and (6), but n in Eq. (9) varies with T. A test of this hypothesis consists in making a comparison of σ and S as in Fig. 3, but now using data at all temperatures instead of only $T = 800\,^{\circ}\mathrm{K}$, and plotting $\log_{10}(800\,\sigma/T)$ instead of $\log_{10}\sigma$ [see Eq. (5)]. When this was done, we indeed found that most of the points lie in the vicinity of the theoretical curve. The exceptions are for data which were measured at unusually high temperatures ($> 900\,^{\circ}\mathrm{K}$) where bipolar transport can be expected in spite of a deep mobility edge in the valence band.

In view of this, it seems to be a good approximation to ignore the contribution of the valence band to the electrical conductivity. This permits us to use the experimental values of $\sigma(T)$ at each composition to infer $n(T)$ at each composition by use of Eqs. (5) and (9), and then to infer from this the hole density $p(T) = n(T) - n_0$. Let us suppose that the valence band is also parabolic, so that we can write

$$N_v(E) = C_p(E_{v0} - E)^{1/2}. \tag{11}$$

Then, in analogy with Eq. (9),

$$p = \int_{-\infty}^{E_{v0}} (1-f) N_v(E)\, dE = C_p(kT)^{3/2} F_{1/2}(\xi_p), \tag{12}$$

where

$$\xi_p = (E_{v0} - E_F)/kT. \tag{13}$$

Since E_{v0} is smaller than E_{c0} by the band gap E_G, $\xi_p = -\xi - E_G/kT$. It is reasonable to assume that E_G varies linearly with T, so we write

$$E_G = E_{G0} - E_{G1}T. \tag{14}$$

Then, using the Maxwell-Boltzmann approximation for ξ_p (which requires that $\xi_p \lesssim -4$), Eq. (12) becomes

$$p = C_p(\tfrac{1}{2}\sqrt{\pi})(kT)^{3/2} \exp(-\xi + E_{G1}/k - E_{G0}/kT)\,. \tag{15}$$

The procedure for analyzing the deviations between the experimental curves for $\sigma(T)$ in Fig. 5 and the theoretical curves based on $n = n_0$ was as follows. For a given composition of Tl_xTe_{1-x} in a range of temperature where the deviations were appreciable, Eq. (5) and (9), together with the previously stated values of AC_n^2k and C_n, were used to calculate ξ and n vs T. An estimate of n_0 was made based on the values at the lowest T, and then a plot was made of $\ln f_p$ vs T^{-1}, where

$$f_p = \frac{(n - n_0)e^{\xi}}{(\frac{1}{2}\sqrt{\pi})\, C_n(kT)^{3/2}}\,.$$

According to Eq. (15), this should yield a straight line with a slope equal to $-E_{G0}/k$ and an intercept equal to $(C_p/C_n)e^{E_{G1}/k}$.

This was done for all available data from this laboratory for which there is appreciable deviation between the $\sigma(T)$ curves and the theoretical curves for constant n. In addition, we used some relatively precise curves obtained by doping Tl_xTe_{1-x} with $x = 0.6686$ with various amounts of indium,[5] making use of the previously established fact that indium atoms provide $\frac{1}{3}$ as many electrons as do thallium.[19] Since the analysis depends on a small difference between large numbers, the original experimental points were used so as to avoid spurious effects caused by smoothing curves. In order to minimize the effect of an arbitrary choice of n_0, the points for relatively small values of $n - n_0$ were ignored. For four compositions with x very close to $\frac{2}{3}$, where thermal excitations were visible at relatively low temperatures, straight lines were obtained with $E_{G0} \cong 0.6$ eV. In the remaining compositions, with increasing values of n_0, straight-line plots were obtained with slopes corresponding to considerably lower values of E_{G0}. We show in Fig. 6 several curves from both categories.

On examining the intercepts for the curves with slopes corresponding to $E_{G0} \cong 0.6$ eV, it became evident that if $C_p/C_n \lesssim 1$, E_{G1} must be of such a magnitude that the band gap becomes negative in the experimental range. This accounts for the second group of curves with low activation energies; p and ξ_p are large enough so that the Maxwell-Boltzmann approximation is not valid, and interpretation of the plots of $\ln f_p$ vs T^{-1} in terms of Eq. (15) is inappropriate.

Using an average of the values obtained from the

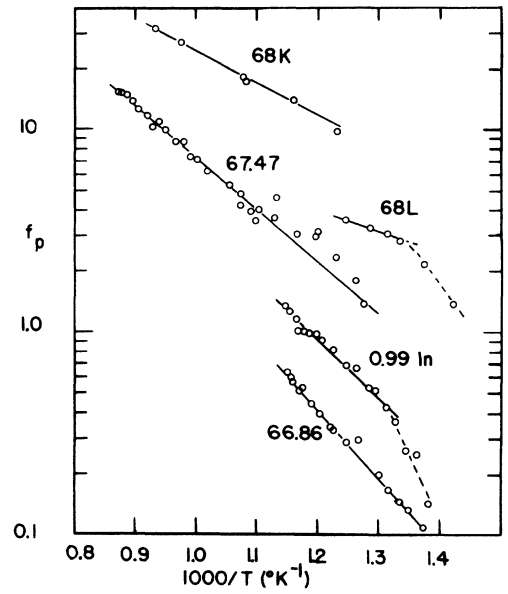

FIG. 6. Several curves for $\ln f_p$ vs T^{-1}. The numbers refer to the composition in at.% Tl except for the one marked In, which is 0.99-at.% indium added to an alloy containing 66.86-at.% Tl.

slopes of the four curves in the first category, we arrive at a value of $E_{G0}=0.58\pm0.02$ eV. In order to determine E_G at any temperature it is necessary to know also E_{G1}. The intercepts would yield this number only if C_p/C_n is specified. Assuming a free-electron effective mass in the valence band leads to a value of E_{G1} which suggests that $E_G=0$ at $T\cong800$ °K. On examining the f_p curves in the second category, it was observed that several of them indeed had sharp breaks near this temperature. The curve marked 0.99 In in Fig. 6 is the most precise of these, and the break occurs at 770 °K. These observations provide a more direct means for determining E_{G1}. Taking 770 °K as the temperature at which $E_G=0$ together with $E_{G0}=0.58$ eV, yields $E_{G1}=7.5\times10^{-4}$ eV °K.

The increases in $n-n_0$ reflected in the f_p curves in the second group are rather large. The fact that they occur for the most part at temperatures above 770 °K, for which $E_{v0}>E_{c0}$, and at compositions in which $E_F>E_{c0}$ suggests the reason for this. Although the states in the valence band at energies below E_{v0} are likely to be localized when the band gap is positive, this cannot continue to be true when they overlap the conduction band, if we are to believe the arguments of Mott.[11] This means that for $T>770$ °K there will be an increase in the density of occupied nonlocalized states which is due to previously nonconducting states of the valence band which are now above $E_{c1}(\sim E_{c0})$. This is illustrated in Figs. 7(a) and 7(b). In addition to this factor, we must consider that according to Eq. (1), $\sigma(E)$ is proportional to the square of the *total* density of states, so that $\sigma(E)$ is larger for the overlapping region than the sum of the contributions of the individual bands, as is shown in Fig. 7(d).

C. Overlapping band model

We are now able to generate a model for transport which includes the thermal effects on σ, but which still assumes monopolar transport (transport by holes at $E<E_{v1}$ is ignored). According to this model, $N(E)$ is taken to be equal to the sum of N_c and N_v given by Eqs. (4) and (11). When this is introduced into Eq. (1), the result is

$$\begin{aligned}\sigma(E)&=AC_n^2(E-E_{c0}) && \text{for } E>E_{v0},\\ &=A[C_n^2(E-E_{c0})+2C_nC_p(E-E_{c0})^{1/2}\\ &\quad\times(E_{v0}-E)^{1/2}+C_p^2(E_{v0}-E)] && \text{for } E_{c0}<E<E_{v0},\\ &=0 && \text{for } E<E_{c0}. \quad (16)\end{aligned}$$

As noted earlier, there is a cross term $2N_cN_v$ in addition to the valence-band contribution N_v^2 when the bands overlap.

On substituting Eq. (16) into Eq. (2), the result is

$$\sigma=AC_n^2kT[F_0(\xi)+2(C_p/C_n)F_{x1}(\xi,x_0)+(C_p^2/C_n^2)F_{x2}(\xi,x_0)], \quad (17)$$

where x_0 is a new parameter equal to $-E_G/kT$. The new definite integrals are

$$F_{x1}=-\int_0^{x_0}x^{1/2}(x_0-x)^{1/2}\,\frac{\partial f}{\partial x}\,dx \quad (18)$$

and

$$F_{x2}=-\int_0^{x_0}(x_0-x)\,\frac{\partial f}{\partial x}\,dx. \quad (19)$$

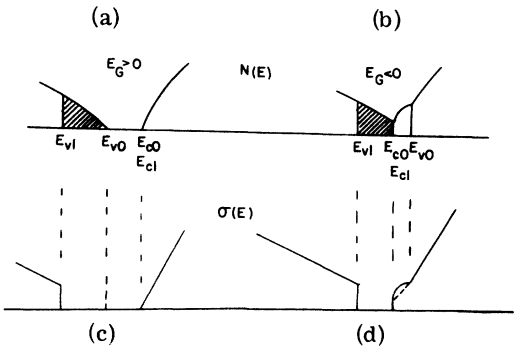

FIG. 7. Two-band-model density of states for a (a) positive and (b) negative band gap. The localized states are indicated by hatching. The corresponding curves for $\sigma(E)$ are shown in (c) and (d). The part above the dashed line in (d) is due to the cross-term N_vN_c in $[N(E)]^2$.

Substituting Eq. (16) into Eq. (3) gives

$$S=\frac{-k}{e}\frac{[2F_1-\xi F_0+2(C_p/C_n)F_{s1}+(C_p^2/C_n^2)F_{s2}]}{F_1+2(C_p/C_n)F_{x1}+(C_p/C_n)^2F_{x2}}, \tag{20}$$

where

$$F_{s1}(x_0,\xi)=-\int_0^{x_0}\frac{\partial f}{\partial x}(x-\xi)x^{1/2}(x_0-x)^{1/2}dx, \tag{21}$$

$$F_{s2}(x_0,\xi)=-\int_0^{x_0}\frac{\partial f}{\partial x}(x-\xi)(x_0-x)dx. \tag{22}$$

The definite integrals F_{x1}, F_{x2}, F_{s1}, and F_{s2} are conveniently evaluated for given values of x_0 and ξ by means of a computer subroutine. [This is also more practical than using tables for the Fermi-Dirac integrals in Eq. (8).]

ξ is now determined by the condition $n-p=n_0$ which yields

$$n_0=C_n(kT)^{3/2}[F_{1/2}(\xi)-(C_p/C_n)F_{1/2}(x_0-\xi)]. \tag{23}$$

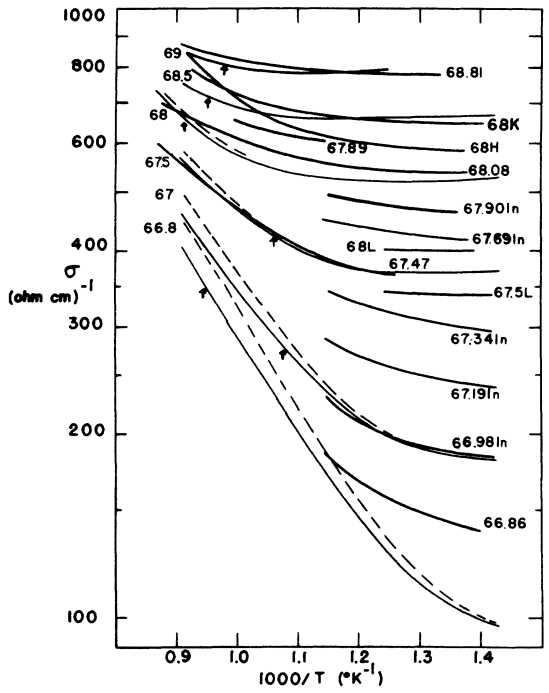

FIG. 8. Comparison of theoretical curves for the overlapping band model with experiment for $\sigma(T)$. The compositions are in at.% Tl and are followed by letters in some cases (H, K, L) to indicate specific runs. Those compositions followed by In are the equivalent compositions in terms of Tl for a 66.86-at.% Tl alloy doped with indium. The monopolar theoretical curves are solid lines marked by small arrows, and have their compositions listed on the left-hand side; the dashed curves indicate the corrections for bipolar transport assuming that $E_s=0.20$ eV and $\sigma_{p1}=0.040$ $(\Omega\ \text{cm}\ ^\circ\text{K})^{-1}$.

It is seen that in addition to the previously determined parameters AC_n^2k, C_n, E_{G0}, and E_{G1}, one must specify one further parameter which we have written as C_p/C_n. This was determined by making computations for arbitrary values of C_p/C_n, and choosing one which gave the best fit to $\sigma(T)$ for a single sample ($x=0.6808$). The computations themselves were carried out by specifying the composition, which determines n_0 [Eq. (10)], and using a computer program to find a value of ξ at each temperature which was consistent with Eq. (23). Then the computer program calculated σ and S according to Eqs. (17) and (20).

Our procedure for determining C_p/C_n led to a value 0.42. The other parameters are $C_n=1.49\times10^{22}$ $\text{eV}^{-3/2}$ cm^{-3}, $E_{G0}=0.58$ eV, $E_{G1}=7.5\times10^{-4}$ eV/°K, and, *initially*, $AC_n^2k=0.2275$ $(\Omega\ \text{cm}\ ^\circ\text{K})^{-1}$. With these parameters, theoretical model curves for $\sigma(T)$ and $S(T)$ were calculated for various compositions. A further improvement in the fit was made by adjusting all of the $\sigma(T)$ curves downward by 10%, which corresponds to adjusting AC_n^2k to 0.206 $(\Omega\ \text{cm}\ ^\circ\text{K})^{-1}$. This reflects the fact that the original value was determined at 800 °K, which is high enough for a small amount of electron-hole excitation to occur. The theoretical curves for $\sigma(T)$ (solid lines marked by small arrows) are compared with experimental curves in Fig. 8. The agreement is, for the most part, within the probable experimental errors. There are some small systematic discrepancies remaining which will be discussed later.

The calculated $S(T)$ curves (solid lines) are compared with experimental points in Fig. 9. The improvement over the extrinsic curves in Fig. 4 is striking. There are small deviations for $x=0.668$ which can be accounted for by a small amount of bipolar transport. It is to be noted that our choices of parameters were based entirely on analysis of the the $\sigma(T)$ curves (aside from the choice of C_n, which sets the composition scale). The large number of parameters which were used might be suspected of providing a fit of data for $\sigma(T)$ which is unrelated to the veracity of the model, but this cannot be so for $S(T)$. Actually, we believe that the wide range of T and x, and consequently the large range of experimental behavior which is covered, as well as the theoretical basis, also argues against this skeptical interpretation for the $\sigma(T,x)$ results.

The results shown in Figs. 8 and 9 show that the overlapping band model provides a good description of σ and S as a function of T in the range $0.67\lesssim x\lesssim0.70$, and corrections for bipolar transport described in Sec. III cause a further improvement. It may be worthwhile to comment here on some tacit assumptions made in the use of the constants in Eqs. (1), (4), (11), and (14). A, C_n, and C_p are in principle all possible functions of the com-

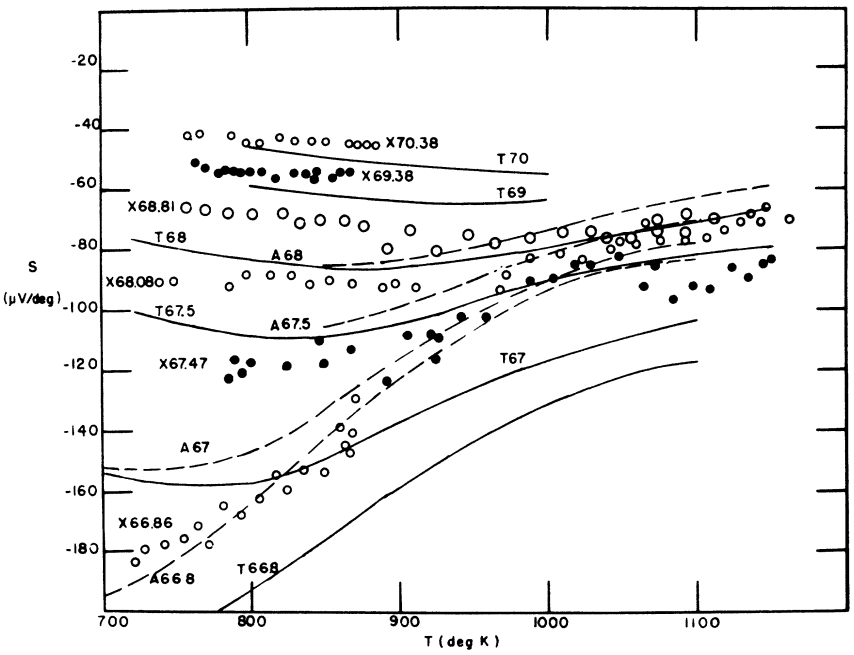

FIG. 9. Comparison of the theoretical thermopower curves (solid and dashed lines) for the overlapping band model with experimental curves (data points indicated by circles). The compositions are in at.% Tl. X indicates experiment, T indicates theoretical (solid) curves for monopolar transport, and A indicates theoretical (dashed) curves with a bipolar correction assuming that $E_s = 0.20$ eV and $\sigma_{p1} = 0.040$ $(\Omega\ \text{cm}\ ^\circ\text{K})^{-1}$.

position. Treating them as constants is of course dictated by the practical need to avoid complicating the model. They may be regarded as the first terms in a power series in x which provides a more accurate description and whose later terms are assumed to be small enough to be neglected. The success of the model supports the validity of this tacit assumption. The same reasoning applies to the use of Eq. (14) for E_G; in this case we keep the first two terms in a power series in T. In addition, there is a physical justification for neglecting the dependence of A, C_p, and C_n on x. The wave functions in the two bands are based largely on the orbitals of Tl_2Te, since the concentration of Tl ions remains relatively small over the range of x in which the model is used. It is therefore reasonable to expect the density of states to be nearly constant. The constant, A depends also on the interatomic distance and the character of the wave functions, which again should not change appreciably.

III. HOLE TRANSPORT

A. Evaluation of the mobility edge

In order to further characterize the pseudogap, it is necessary to determine the energy interval between the valence band edge E_{v0} and the mobility edge E_{v1}, which we shall call E_s. Because of the particular structure of $\sigma(E)$ near E_{v1}, as shown in Fig. 7(c), and the diffuseness of the Fermi-Dirac function f at these high temperatures, one would expect that the largest sensitivity of σ to the position of E_{v1} will occur when E_F is near E_{v1}. Therefore we look to transport data for $x \lesssim \frac{2}{3}$ for information bearing on this question.

It is not possible for several reasons to carry out an analysis of thermal excitation effects in the valence band as directly as that described in Sec. II for the conduction band. First, the transport due to electron-hole excitations is bipolar. Second, the mobility edge complicates the expression for σ by introducing another parameter $E_s (= E_{v0} - E_{v1})$. And finally, the situation in the absence of electron-hole pairs cannot be characterized by a constant hole density. σ and S change rapidly with T at p-type compositions well away from $x = \frac{2}{3}$ in a way which indicates that the hole concentration increases with T. The author believes that this is caused by the rupture of Te-Te bonds in chain molecules of the structure Tl-Te_n-Tl. In an earlier paper,[7] an analysis of the transport behavior for $x < \frac{2}{3}$ was presented in terms of this mechanism. Although the author believes that the analysis supports his interpretation, it contains too many discrepancies and arbitrary elements for it to be used as a reliable starting point for the present study.

It was possible to obtain an estimate of E_s by a rather complicated procedure which shall be described below. It contains several arbitrary elements which the author thinks have little effect on the final result. The procedure will be described first and then the questionable elements in it will be discussed.

The starting point is a series of experimental curves for $\sigma(T)$ in the composition range $x \lesssim \frac{2}{3}$ which are close enough to Tl_2Te and at high enough temperatures for electron-hole excitations to cause

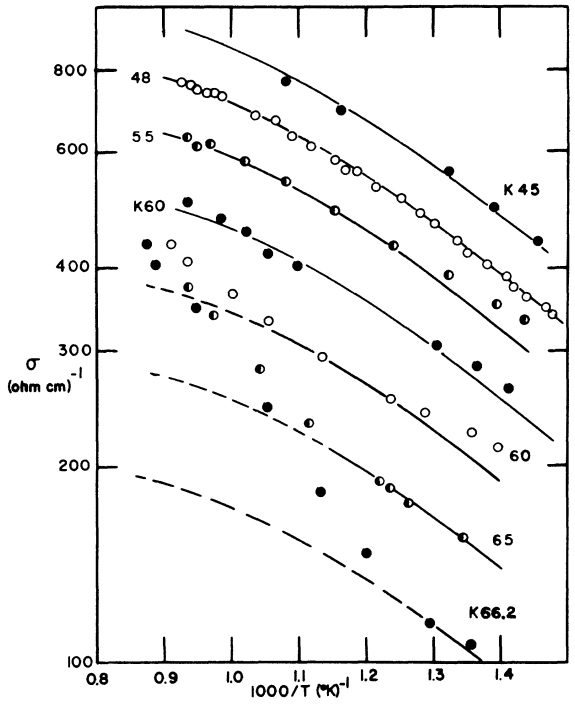

FIG. 10. Experimental $\sigma(T)$ curves for compositions $x < \frac{2}{3}$. The solid lines indicate the matched empirical curve $\sigma_p^0(T)$, with the dashed extensions to indicate the regions where $\sigma(T)$ rises above the empirical curve because of thermal excitations. The compositions are indicated in terms of $100x$. The curves marked K are from Ref. 22, and the rest are from this laboratory.

appreciable deviations from the extrinsic behavior. Figure 10 shows a number of these curves as well as some at compositions where only the extrinsic behavior occurs. As noted in an earlier paper,[8] the extrinsic curves for $\log_{10}\sigma$ vs T^{-1} fall very accurately on a common curve. For the present purpose, this is best expressed by the empirical function

$$\sigma_p^0 = \sigma_1 (1000/T)^{2.54} e^{-3540/T}. \tag{24}$$

By fitting this curve at each composition to the experimental curve at the low-temperature end where electron-hole excitations are small, we determine a value of the constant σ_1 and then calculate $\sigma - \sigma_p^0$ vs T from the original data points. For this purpose, we have used data at $x \gtrsim 0.60$ from this laboratory[8,20,21] and also data reported by Kazandzhan *et al.*[22]

Let us first outline briefly the path to be followed. We infer from $\sigma - \sigma_p^0$, at least approximately, the contribution σ_n due to the electrons in the conduction band. Then the transport equations of Sec. II are used to derive from this the distance of the Fermi energy E_F from the conduction band edge E_{c0}. With the known dependence of E_G on T, this is converted into $E_{v0} - E_F$. Since we know the extrinsic conductivity $\sigma_p^0(x, T)$, we pick a single temperature (1000 °K) and plot $E_{v0} - E_F$ vs σ_p^0. By comparing this with a series of theoretical curves derived from a mobility shoulder model for σ vs $E_{v0} - E_F$ for various values of E_s, we arrive finally at an estimate of the correct value of E_s.

The first problem is to infer σ_n from $\sigma - \sigma_p^0$. Since $\sigma - \sigma_p^0$ is equal to $\Delta\sigma_p + \sigma_n$, we cannot separate the contribution of $\Delta\sigma_p$ without using a complex procedure requiring introduction at an early stage of a model for conduction in the valence band. But since the number of electrons responsible for σ_n is equal to the number of holes responsible for $\Delta\sigma_p$, it is a fair approximation to assume that σ_n and $\Delta\sigma_p$ are in a fixed ratio, so that σ_n is some fraction of $\sigma - \sigma_p^0$. We assume that this fraction is $\frac{1}{2}$.

The next step is to infer $E_{c0} - E_F$. The temperature range in which $\sigma - \sigma_p^0$ is large is mainly in the vicinity of 1000 °K, where the bands overlap appreciably. The use of Eq. (17) to infer ξ from σ_n would require complicated calculations not justified because of the other approximations. Therefore we ignore the overlapping band contributions for the present purpose and use instead Eq. (5). In Fig. 11 some representative curves are plotted for $E_{c0} - E_F$ vs T obtained in this way.

It is interesting to note that the points tend to lie on a straight line with the same slope $-E_{G1}$ as the band gap. This is somewhat surprising since one would expect $E_{v0} - E_F$ to change with temperature as well as $E_{c0} - E_{v0}$. We shall discuss this point later. For the present purpose, we use a straight-line plot with a slope $-E_{G1}$ only in order to interpolate (or extrapolate, in one case) and determine the value of $E_{c0} - E_F$ at $T = 1000$ °K for each composition. Then, using the previously determined dependence of E_G on T, we subtract $E_{c0} - E_{v0}$

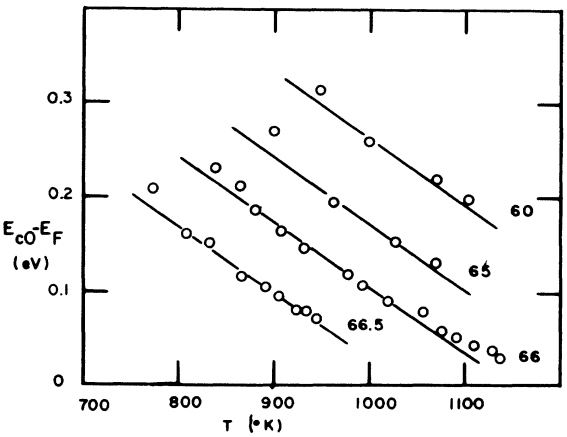

FIG. 11. Some curves for $E_{c0} - E_F$ vs T deduced from $\sigma - \sigma_p^0$ for various compositions, indicated in terms of $100x$.

$= -0.173$ eV in each case to obtain $E_{v0}-E_F$. These data are divided by kT ($=0.0862$ eV) and are plotted as ξ_p in Fig. 12 with the corresponding values of $\log_{10}\sigma_p^0$ as the ordinate.

We can now compare these results with a theoretical curve for $\log\sigma$ as a function of $E_{v0}-E_F$ derived from a simple model for $\sigma(E)$, assuming again a parabolic density of states with the conductivity cut off for $E > E_{v1}$:

$$\sigma(E)=0 \qquad \text{for } E>E_{v1}$$
$$\sigma(E)=A_pC_p^2(E_{v0}-E) \quad \text{for } E<E_{v1}. \tag{25}$$

On substituting this into Eq. (2), one obtains

$$\sigma_p=A_pC_p^2kT\,F_p(\xi_p,x_c). \tag{26}$$

F_p is a truncated Fermi-Dirac function of ξ_p [Eq. (13)] and of x_c, which is equal to $(E_{v0}-E_{v1})/kT$:

$$F_p(\xi_p,x_c)=-\int_{x_c}^{\infty} x\,\frac{\partial f}{\partial x}\,dx$$
$$=\frac{x_c}{e^{x_c-\xi_p}+1}+\ln\,(1+e^{\xi_p-x_c}). \tag{27}$$

We have plotted σ_p vs ξ_p in Fig. 12 for several values of x_c. In doing this we set the constant $A_pC_p^2k=0.072$ $(\Omega\,\text{cm}\,^\circ\text{K})^{-1}$. (We shall refer to this constant as σ_{p1}.), which seems to provide the best fit with the experimental points. The vertical positions of the theoretical curves are insensitive to x_c at large values of ξ_p, so that the points at $\xi_p \gtrsim 4$ essentially determine the value of σ_{p1}. Most of the points at lower values of ξ_p lie near the curve for $x_c=3$. The lowest point deviates considerably. But since this composition is very close to intrinsic it is likely that σ_p^0 was set too high in this case when fitting the experimental data to Eq. (24). The value $x_c=3$ corresponds to $E_s=0.26$ eV.

Let us now consider the approximations which were used in the foregoing analysis. First, the ratio $\phi=\sigma_n/(\sigma-\sigma_p^0)$ is not likely to be equal to $\frac{1}{2}$ nor to be constant. However, the values of $E_{c0}-E_F$ are in a range where the Maxwell-Boltzmann approximation to Eq. (5) is nearly valid, so that a change $\delta\ln\phi$ results in a change in $E_{c0}-E_F$ of the order $kT\delta\ln\phi$. Thus an error in ϕ by a factor of 2 would cause a shift in $E_{c0}-E_F$ of less than kT, and a moderate change in ϕ with T would cause a small change in this quantity. Since it seems very likely that ϕ will be within the range $\frac{1}{4}-1$, we expect relatively small errors in $E_{c0}-E_F$, less than ~ 0.05 eV.

Another approximation was to ignore the changes in $\sigma(E)$ of the conduction band due to band overlap. Because we are nearly in the Maxwell-Boltzmann range for Eq. (5), $E_{c0}-E_F$ can be expressed as $kT\ln(\sigma_T/\sigma_n)$, where σ_T is an average of $\sigma(E)$ mainly within a distance kT of the band edge. σ_T would be larger than what was assumed by roughly a factor of 2, so that $E_{c0}-E_F$ would be too small by roughly 0.05 eV. Since approximately the same temperature range was used in each of the curves in Fig. 11, they would all be displaced by approximately the same amount. If the factor ϕ in the preceding paragraph is greater than $\frac{1}{2}$, which is what we expect, these errors would tend to cancel. (Since both errors are proportional to T, there will also be an error in the slope. We discuss this factor below.)

As mentioned earlier, the straight line plots in Fig. 11 with the slope $-E_{G1}$ is used in our analysis essentially to determine the dependence of $E_{c0}-E_F$ on composition at a fixed T, which information is used in the subsequent analysis. However, the fact that $d(E_{c0}-E_F)/dT$ agrees with dE_G/dT which implies that $E_{v0}-E_F$ is independent of temperature, and this deserves some comment. Over the temperature range which is used in Fig. 9, σ_p^0 changes by a factor 1.4. By using our theoretical curve described by Eq. (27) with $x_c=3$, we can infer from this the change in $E_{v0}-E_F$ over this temperature range ($\sim$ 800–1000 °K). The result depends somewhat on the composition, but it corresponds roughly to $d(E_{v0}-E_F)/dT \cong +3.5\times10^{-4}$ eV/°K. Since $E_{G1}=7.5\times10^{-4}$ eV/°K, one would therefore expect that $d(E_{c0}-E_F)/dT \cong -4\times10^{-4}$ eV/°K. The approximations of ignoring the over-

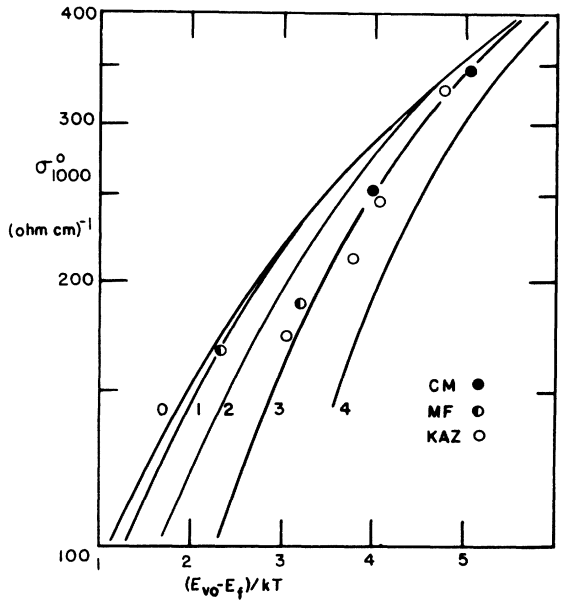

FIG. 12. Experimentally deduced values of σ_p^0 vs ξ_p at 1000°K are compared with theoretical curves based on Eq. (26), with $A_pC_p^2k$ set at 0.072 $(\Omega$ cm °K$)^{-1}$, and with integral values of x_c from 1 to 4. Sources of data are Ref. 8 (CM), Ref. 21 (MF), and Ref. 22 (KAZ).

lapping band effect and assuming $\phi = \frac{1}{2}$, discussed in the preceding paragraph, could decrease the slope, but only by an amount of the order of k or $\lesssim 1\times10^{-4}$ eV/°K, so that this is not enough to account for the discrepancy. We emphasize that the dependence of $E_{c0}-E_F$ on T entered only in a very minor way into the method used for arriving at the value of E_s. But the lack of self-consistency of the final result is something to be concerned about.

Let us finally consider the magnitude of σ_{p1} ($=A_pC_p^2k$) derived from Fig. 12. This value 0.072 (Ω cm °K)$^{-1}$ differs from the value 0.040 (Ω cm °K)$^{-1}$ inferred from the analysis in Sec. II. A simple interpretation is that A_p/A has the value 1.8, rather than unity assumed in Sec. II. Values for the constant A in Eq. (1) which differ by such a factor for the two bands is quite consistent with the basic theory, and could be the result of a smaller coordination number for the valence-band wave functions.[23] But a complication arises in the choice of a suitable constant for the overlapping band region, if one wanted to make a consistent model; we shall discuss this problem later. An alternative interpretation is that A is the same but C_p is larger. Such an effect can be expected if $N_v(E)$ is not truly parabolic, but increases more rapidly than the one-half power of $E_{v0}-E$. The analysis of this section deals with a situation where E_F is well within the valence band, whereas in Sec. II E_F is generally above E_{v0}. Thus our arbitrary parabolic band model would project a different value of C_p depending on the position of E_F. This sort of distortion from a parabolic shape is also a reasonable possibility.

B. Bipolar transport for $x \geq \frac{2}{3}$

The added contributions to σ and S in the n-type region due to holes provide small corrections to the results of Sec. II, but factors considered in the preceding paragraph cause complications in calculating them. Let us consider first the simplest procedure, which is to use the parameter for σ_{p1} deduced in Sec. II, and calculate the bipolar correction using only the estimate of the mobility edge E_{v1} obtained in Sec. III A.

The bipolar thermopower is $S_b = (\sigma S + \sigma_p S_p)/(\sigma+\sigma_p)$, where S and σ are given by Eqs. (20) and (17), respectively. From Eqs. (3) and (25),

$$\sigma_p S_p = (k/e)\, A_p C_p^2 kT\,[F_{sp}(x_c', \xi_p) - \xi_p F_p(x_c', \xi_p)] \tag{28}$$

where

$$F_{sp} = \int_{x_c'}^{\infty} x(x-\xi_p)\,\frac{-\partial f}{\partial x}\,dx. \tag{29}$$

x_c' is the same as $(E_{v1}-E_{v0})/kT$ with the exception that when T is high enough so that E_{v1} is greater than E_{c0}, E_{v1} is replaced by E_{c0} in order to avoid counting twice the region of $\sigma(E)$ where $E_{c0}<E<E_{v1}$. (Note that this correction is accurate only if $A_p = A$.) Similarly, the bipolar electrical conductivity is $\sigma_b = \sigma + \sigma_p$, where σ_p is given by Eq. (26) with the argument x_c' instead of x_c.

These corrections were calculated for $E_s = 0.2$ eV, and with σ_{p1} equal to 0.040 (Ω cm °K)$^{-1}$ as determined in Sec. II. The bipolar curves for σ and S are shown in Figs. 8 and 9 as dashed lines. As one would expect, the correction becomes small as x departs from the value $\frac{2}{3}$. At the lowest thallium concentration, $x = 0.668$, S changes appreciably, and the theoretical curve comes into good agreement with experiment. We point out, however, that the bipolar corrections, which are rather small on the whole, would not be much larger if we were to let $E_s = 0$ rather than 0.2 eV. That is, for σ and S at $x > \frac{2}{3}$, the fact that there is a mobility shoulder in the valence band has little visible effect for this value of σ_{p1}.

The most sensitive composition for examination of the accuracy of our bipolar model is at x exactly equal to $\frac{2}{3}$. Some rather precise and detailed data

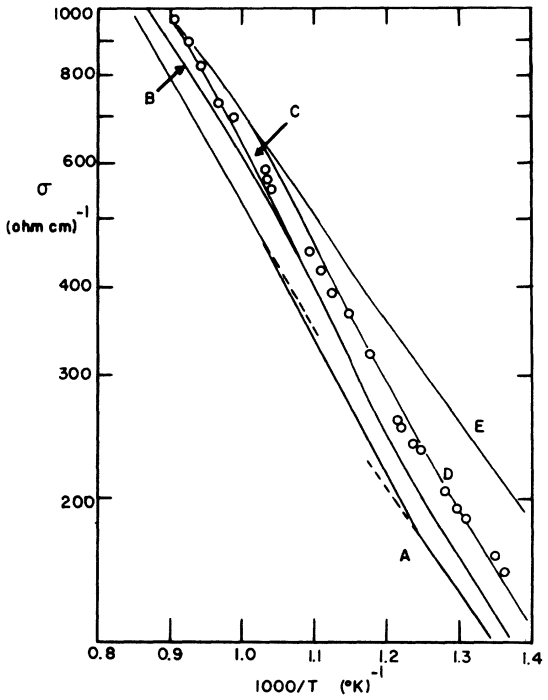

FIG. 13. Comparison of theoretical curves of $\sigma(T)$ with experimental points (circles) from data of Ref. 22. Curve A is the monopolar result, with the dashed extensions of high- and low-T parts to emphasize the inflection. The remaining curves include bipolar corrections with the following parameters: Curve B has $\sigma_{p1} = 0.040$ (Ω cm °K)$^{-1}$ and $E_s = 0.20$ eV. Curves C, D, and E have $\sigma_{p1} = 0.072$ (Ω cm °K)$^{-1}$ with $E_s = 0.26$, 0.17, and 0 eV, respectively.

for $\sigma(T)$ have been reported at this composition (Tl_2Te) by Kazandzhan *et al.*[22] which are in agreement with less detailed curves determined at our own and other laboratories. These data are shown in Fig. 13, together with our theoretical curves derived from the overlapping band model for both the monopolar (curve A) and bipolar (curve B) calculation described above. It is seen that the monopolar result is in substantial agreement with experiment (within 20%), and the bipolar result removes a large part of this small discrepancy. The fact that the intrinsic curve with its strong temperature dependence is quite different in character from the largely extrinsic curves in Fig. 8 again makes it unlikely that the success of our model is merely caused by curve fitting with a large enough number of parameters.

Another interesting thing about the results in Fig. 13 is that both the theoretical and experimental curves show a distinct inflection and change in slope near $T \sim 900\,^\circ\mathrm{K}$. This is emphasized by dashed extensions of the low- and high-temperature sections of curve A. This mainly reflects the effect of the overlapping band on $\sigma(E)$ which occurs for $T > 770\,^\circ\mathrm{K}$. Such an inflection occurs, although somewhat reduced, even if we assume no mobility shoulder ($E_s = 0$), so that its presence does not prove the existence of a mobility shoulder.

It is possible to compute bipolar corrections assuming that $\sigma_{p1} = 0.072\ (\Omega\,\mathrm{cm}\,^\circ\mathrm{K})^{-1}$ as inferred from the analysis of Sec. III A, instead of $0.040\ (\Omega\,\mathrm{cm}\,^\circ\mathrm{K})^{-1}$. There is in this case an ambiguity about the contribution of the overlapping states when E_{v1} exceeds E_{c0} at high temperatures, but this is a small effect added to a small correction. If we make this calculation, using $E_s = 0.26$ eV, the resulting curve C is practically identical to curve B in Fig. 13, running slightly higher at high temperatures. Since this value for E_s is not a precise one, it makes sense to consider what value gives best agreement with the experimental points. A value of $E_s = 0.17$ eV matches the experimental points at low T, but runs somewhat higher at high T, as shown in Fig. 13 by curve D. We show also (curve E) the result assuming $E_s = 0$, which differs significantly from the experimental curve.

Of course, the use of a larger value of A_p for the bipolar correction is inconsistent with use of Eq. (16) for the electron contribution to $\sigma(E)$. It would be desirable to examine a consistent solution for σ and S when $A \neq A_p$. It is not obvious what is the correct expression for A in Eq. (1) for overlapping bands when it has different values for the separate bands. But it seems reasonable and it is also mathematically convenient to use the geometric mean for the cross term $2N_vN_c$. Thus we modify Eq. (16) for the overlapping band region ($E_{c0} < E < E_{v0}$) by replacing A by A_p for the third term, and by $(A_pA)^{1/2}$ for the second term. This has the effect of replacing the factors (C_p/C_n) by $(C_p/C_n) \times (A_p/A_n)^{1/2}$ in Eq. (17) for σ and Eq. (20) for S. But the factor (C_p/C_n) in Eq. (23), which determines the Fermi energy, remains the same. The reader will recall that a value $(C_p/C_n) = 0.42$ provided the best fit of the theoretical curves in the original monopolar calculation. Replacing this in Eq. (17) and (20) by 0.59, as implied by a ratio $A_p/A = 1.8$, would destroy the good agreement between theory and experiment which is shown in Figs. 8 and 9 for $x > \frac{2}{3}$. The σ curves increase too rapidly at high T, and the magnitude of S would fall significantly below the experimental curves. One might hope to compensate for this by also changing the value of the independently disposable parameter C_p/C_n in Eq. (23). But it turns out that the results are very weakly dependent on this parameter, and one cannot get agreement with experiment for $(C_p/C_n)(A_p/A_n)^{1/2} = 0.59$ for any physically reasonable value of C_p/C_n. The fact that one cannot arrive at a self-consistent model for the electron contribution when the hole contribution has a value determined by $\sigma_{p1} = 0.72\ (\Omega\,\mathrm{cm}\,^\circ\mathrm{K})^{-1}$ supports the interpretation that $N_v(E)$ is not parabolic.

Let us now consider $S(T)$ for $x = \frac{2}{3}$. Kazandzhan *et al.*[22] report a curve shown in Fig. 14, which saturates at high T at $\sim -45\ \mu\mathrm{V}/^\circ\mathrm{K}$. Curves have also been obtained in our laboratory for near-intrinsic compositions which differ at lower T but also tend to saturate at the same value at high temperatures. One of these is also shown in Fig. 14. Since the behavior of S at lower T is extremely sensitive to small deviations from the intrinsic composition, we may take the high-T limit to be the more significant experimental result.

The theoretical curves for $x = \frac{2}{3}$ are very sensitive to the bipolar contribution. The monopolar curve (A in Fig. 14) differs considerably from the experimental ones. Curve B which includes a bipolar correction based on $\sigma_{p1} = 0.040\ (\Omega\,\mathrm{cm}\,^\circ\mathrm{K})^{-1}$ and $E_s = 0.20$ eV [corresponding to curve B for $\sigma(T)$ in Fig. 13] is a considerable improvement, and saturates at $\sim -80\ \mu\mathrm{V}/^\circ\mathrm{K}$. Curves C, D, and E are for $\sigma_{p1} = 0.072\ (\Omega\,\mathrm{cm}\,^\circ\mathrm{K})^{-1}$ with $E_s = 0.26$, 0.17, and 0 eV, respectively [corresponding to curves C, D, and E for $\sigma(T)$ in Fig. 14]. Here the saturation value is $\sim -55\ \mu\mathrm{V}/^\circ\mathrm{K}$, which is rather good agreement with experiment. We should note, however, that these bipolar corrections to S, which gives the better result for $x = \frac{2}{3}$, gives a poorer result for $x = 0.668$ than the one shown in Fig. 9.

To summarize the rather involved discussion in this section, a mobility shoulder analysis of the thermal excitations on $\sigma(T)$ for near-intrinsic p-type compositions leads to an estimate for the position of the mobility edge E_s which is several

times larger than kT. It also leads to a conductivity parameter σ_{p1} for the valence band which is nearly twice as large as the one deduced in Sec. II. Inclusion of bipolar effects materially improves the agreement with experiment for S and σ at $x = \frac{2}{3}$ and $x = 0.668$. However, one cannot arrive at a form of $\sigma(E)$ for $E > E_{c0}$ in the overlapping band domain which is consistent with the results of the mobility shoulder analysis without destroying the agreement with experiment for compositions more highly doped with thallium.

IV. DISCUSSION

The model which we have developed for transport in Tl-rich compositions still has several limitations worth noting. First, it fails to describe correctly thermal excitation effects which apparently occur for $x \gtrsim 0.71$, particularly in the dependence of S on T. We have noted in an earlier paper[6] that $S(T)$ deviates from a behavior expected for constant electron density ($S \propto T$) when $x \lesssim 0.75$. Because E_F remains high compared to E_{v0} in the experimental temperature range for $x \gtrsim 0.70$, the overlapping band model does not predict an appreciable change from the constant electron density result. This cannot be overcome by moderate changes in the parameters of the model.

Of course, it is too much to expect some aspects of our model, such as the density-of-states curve, to continue to be correct as the composition is changed drastically and the Fermi energy rises well into the conduction band. But this could not account for the discrepancy, which relates to the effect of temperature. The most likely cause, we think, is the dissociation of a small fraction of the Tl-Te bonds. Near the composition Tl_2Te, the conduction band is expected to be generated primarily from antibonding orbitals of Tl-Te bonds.[7] If the conduction band were a tight-binding band generated entirely from these antibond orbitals, there would be no binding energy when this band is filled, and the binding energy would decrease as the Fermi energy increases. The conduction band is not a tight-binding band; it includes and is generated in part from other orbitals, including those of the extra Tl atoms. This becomes increasingly true at higher energies in the band and as the thallium concentration increases. It is reasonable, nonetheless, to expect an increasing fraction of the Tl-Te bonds to dissociate at high T as E_F increases with increasing x. But at the same time, the ratio of Tl_2Te molecules to excess Tl atoms decreases, so that at some point the effect of bond dissociation in increasing the electron density should become submerged by the high electron density due to the Tl atoms. This ratio drops below one when x exceeds 0.75, and this happens to be also the point at which thermal excitations cease to be visible.

There are several other discrepancies which may be attributed to deviations of the valence-band density of states from the parabolic shape assumed in our model. The theoretical curves for $\sigma(T)$ level off and tend to increase as T decreases below 770 °K, for $x \gtrsim 0.675$. On the other hand, there is a tendency for the experimental curves to decrease slightly in this range. This suggests that there is some tailing of the valence band with the result that there is still some band overlap for $T < 770$ °K. We have discussed in Sec. III evidence of a distortion of the valence band from a parabolic shape, as indicated by values of C_p which differ for different ranges of E_F. Band tailing and distortion from a parabolic shape deeper in the valence band are apt to go together.[10]

Another way to resolve discrepancies which seem to require different values of C_p for different composition ranges is to drop or diminish the second term $2N_cN_v$ in the quadratic expression for $[N(E)]^2$ [Eq. (16)]. This might be justified theoretically if the states of the two bands differ greatly in character, so that they do not mix strongly when the bands overlap. Such a hypothesis would permit the use of a larger ratio of C_p/C_n in fitting the high-T parts of the monopolar $\sigma(T)$ curves in thallium-rich compositions, and would perhaps yield better agreement with results derived for compositions at $x < \frac{2}{3}$. It would be possible to extend the model to include either of the

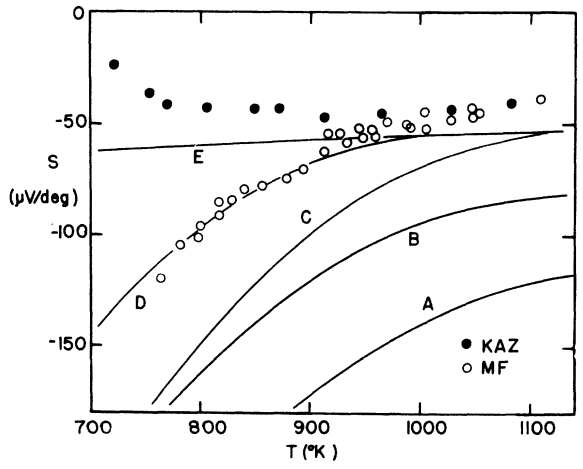

FIG. 14. Comparison of theoretical curves of $S(T)$ with experiment for $x = \frac{2}{3}$. The data marked KAZ are from Ref. 22. Those marked MF, from Ref. 21, are for an alloy at $x = 0.665$ to which a small amount of indium was added. The parameters for theoretical curves A, B, C, D, and E are described in Fig. 13.

above explanations. However, the discrepancies to be accounted for are small and additional parameters would need to be introduced, so that such an effort does not seem to be warranted at the present time.

Experimental evidence for the occurrence of mobility shoulders in amorphous solids has been the subject of considerable interest because of theoretical disagreements[13] about their nature. It is a matter of interest then to examine the extent to which our results prove the existence of a mobility edge in Tl-Te. As already noted, we have evidence that it is not far enough from the band edge to be visible in the conduction band. Evidence for its occurrence in the valence band falls into three categories which we shall discuss in turn.

First, we used the putative existence of a deep mobility edge to justify a monopolar analysis of the thermal excitations in compositions $x > \frac{2}{3}$ in Sec. II B. However, the model ultimately derived shows that the main thermal effect arises from the increase in $[N(E)]^2$ for conducting states which occurs when $T > 770\,^\circ\mathrm{K}$, and the maximum possible contribution due to states at energies below E_{c0} is relatively small.

The second piece of evidence is the analysis of the thermal excitations for $x < \frac{2}{3}$, which led to the comparison with theoretical curves for a mobility edge shown in Fig. 12. The comparison of theory and experiment seems to provide distinct evidence of a mobility edge. But this conclusion is marred by the occurrence of some inconsistencies which we have discussed in Sec. III. Probably the most disturbing element here is the evidence that the valence band may deviate from a parabolic shape. The deviation is in a direction which would cause a steeper slope of the theoretical curve for $E_s = 0$ in Fig. 12 which would lead to better agreement with the experimental curve. So without examining specific models for a nonparabolic band edge we cannot be sure that the observed slope requires the existence of a mobility edge.

The third source of inference about the mobility edge consists in the comparison of the bipolar curves with experiment for compositions at or near $x = \frac{2}{3}$, since the magnitude of E_s enters into the bipolar corrections. We show in Figs. 8 and 9 bipolar curves calculated with $\sigma_{p1} = 0.040$ $(\Omega\,\mathrm{cm}\ ^\circ\mathrm{K})^{-1}$ and $E_s = 0.2$ eV. If they are calculated instead with $E_s = 0$, the results are practically the same, so that this leads to no conclusion about the mobility edge. The reason for this insensitivity is the small value of σ_{p1} relative to AC_n^2k. We also examined the bipolar effect for $\sigma_{p1} = 0.072$ $(\Omega\,\mathrm{cm}\ ^\circ\mathrm{K})^{-1}$, as suggested by the mobility-edge analysis. In this case, there is greater sensitivity to the value of E_s. A zero value for E_s causes the theoretical curve (E) for $\sigma(T)$ in Fig. 13 to be appreciably higher than the experimental curve at low T ($\sim 30\%$), whereas values of 0.17 eV (curve D) and 0.26 eV (curve C) are in better agreement. With regard to $S(T)$, the limiting high-T value of S for $x = \frac{2}{3}$ is independent of E_s, but the low-temperature part of the curve is strongly affected, with lower values causing saturation to occur at lower temperature. Curves C, D, and E in Fig. 14 are roughly consistent with experimental curves at low T because of sensitivity of the latter to composition.

Taking these various considerations together, we conclude that there is considerable evidence for a mobility edge at $E_s \simeq 0.2$ eV, but it is not conclusive.

Our conclusions about the positions of the mobility edges in relation to $\sigma(E)$ are consistent with Mott's discussions of the subject. He has estimated that $\sigma(E)$ at the mobility edge should be $\sigma_c \sim 100$–200 $(\Omega\,\mathrm{cm})^{-1}$, depending on the character of the wave functions and the coordination number.[11,15] For the conduction band, our value of AC_n^2k leads to $\sigma_c \sim 180$ $(\Omega\,\mathrm{cm})^{-1}$ at a distance kT above the band edge. Thus our conclusion that $E_{C1} - E_{C0} \gtrsim kT$ agrees with Mott's estimate. Because of the low value of C_p/C_n, the Mott estimate requires a deeper mobility edge for the valence band, and indeed the value of σ_{p1} derived in Sec. III A leads to $\sigma(E_{v1}) = 208$ $(\Omega\,\mathrm{cm})^{-1}$ for $E_s = 0.26$ eV.

It is worth emphasizing here the general implications of the fact that the distances of the mobility edges from the band edges are not likely to be equal in any disordered material. As noted previously by Mott and Davis,[3] this makes it unlikely that bipolar transport will occur for intrinsic materials, and also on one of the two sides of the intrinsic composition. This fact, which has been overlooked in a number of recent papers, has greater impact in amorphous solids than in liquids because of the small value of kT.

In summary, we have developed a model for the pseudogap, expressed in terms of two bands with a temperature-dependent band gap, which succeeds in very large measure in accounting for the temperature dependence of S and σ for Tl_xTe_{1-x} in the composition range $0.667 \leq x \leq 0.70$. In terms of this model, the band gap has a large negative temperature coefficient ($E_{G1} \sim 7.5 \times 10^{-4}$ eV/°K) and it becomes negative for $T > 770\,^\circ\mathrm{K}$. These results are similar to those deduced for liquid As_2Se_3.[2,3] In carrying out this analysis, we have made fruitful use of the concepts developed by Mott regarding the nature of diffusive transport in relation to the density of states. The possible occurrence of mobility edges has been examined, and we find evidence that it is small in the conduction band ($E_{c1} - E_{c0} \gtrsim kT$), and derived a rough value for the valence band ($E_{v0} - E_{v1} \sim 0.2$ eV). But the evidence for the latter is ambiguous.

[1]J. N. Hodgson, Phil. Mag. 8, 735 (1963).
[2]J. T. Edmund, Brit. J. Appl. Phys. 17. 979 (1966).
[3]N. F. Mott and E. A. Davis, *Electronic Processes in Non-Crystalline Materials* (Clarendon, Oxford, England, 1971).
[4]J. Tauc and A. Abraham, Helv. Phys. Acta 41, 1225 (1968).
[5]M. Cutler and M. B. Field, Phys. Rev. 169, 632 (1968). This paper will be referred to as CF.
[6]M. Cutler and R. L. Petersen, Phil. Mag. 21, 1033 (1970).
[7]M. Cutler, Phil. Mag. 24, 381 (1971).
[8]M. Cutler and C. E. Mallon, Phys. Rev. 144, 642 (1966).
[9]A more complete exposition of this theory is to be found in Ref. 3.
[10]B. I. Halperin and M. Lax, Phys. Rev. 148, 722 (1966).
[11]N. F. Mott, Phil. Mag. 17, 1259 (1968); Phil. Mag. 22, 1 (1970).
[12]P. W. Anderson, Phys. Rev. 109, 1492 (1958).
[13]D. J. Thouless, J. Non-Crystalline Solids 8-10, 461 (1972).
[14]M. H. Cohen, J. Non-Crystalline Solids 4, 391 (1970).
[15]N. F. Mott, Phil. Mag. 19, 835 (1969).
[16]N. K. Hindley, J. Non-Cryst. Solids 5, 17 (1970).
[17]W. W. Warren, Jr., Phys. Rev. B 3, 3708 (1971).
[18]M. Cutler, Phil. Mag. 25, 173 (1972).
[19]M. Cutler, Solid State Commun. 13, 1293 (1973).
[20]C. E. Mallon and M. Cutler, Phil. Mag. 11, 667 (1965).
[21]M. B. Field, M. A. thesis (Oregon State University, 1967) (unpublished).
[22]B. I. Kazandzhan, A. A. Lobanov, Yu. I. Selin, and A. A. Tsurikov, Fiz. Tekh. Poluprovodn. 5, 1625 (1971) [Sov. Phys.-Semicond. 5, 1419 (1972)].
[23]L. Friedman, J. Non-Cryst. Solids 6, 329 (1971).